AMERICAN SOCIETY FOR MICROBIOLOGY | Antimicrobial Agents and Chemotherapy®

EXPERIMENTAL THERAPEUTICS

Biocompatibility and Targeting Efficiency of Encapsulated Quinapyramine Sulfate-Loaded Chitosan-Mannitol Nanoparticles in a Rabbit Model of Surra

Anju Manuja,[a] Balvinder Kumar,[a] Rajender Kumar,[a] Meenu Chopra,[a] Neeraj Dilbaghi,[b] Sandeep Kumar,[b] Suresh C. Yadav[a]

[a]ICAR–National Research Centre on Equines, Hisar, Haryana, India

[b]Department of Bio & Nano Technology, Guru Jambheshwar University of Science and Technology, Hisar, Haryana, India

ABSTRACT Quinapyramine sulfate (QS) produces trypanocidal effects against the parasite *Trypanosoma evansi* but is often poorly tolerated and causes serious reactions in animals. The encapsulation of QS in chitosan-mannitol to provide sustained release would improve both the therapeutic effect of QS and the quality of life of animals treated with this formulation. QS was encapsulated into a nanoformulation prepared from chitosan, tripolyphosphate, and mannitol nanomatrix (ChQS-NPs). ChQS-NPs were well ordered in shape, with nanoparticle size, as determined by transmission electron microscopy and atomic force microscopy. Our research revealed dose-dependent effects on biosafety and DNA damage in mammalian cells treated with ChQS-NPs. ChQS-NPs were absolutely risk-free at effective as well as many times higher doses against *T. evansi*. ChQS-NPs were effective in rabbits, as they killed the parasites, relieving the animals from the clinical symptoms of the disease. The extent of this protection was similar to that observed with the conventional drug at higher dosages (5 mg QS/kg of body weight). ChQS-NPs are safe, nontoxic, and more effective than QS and offer a promising alternative to drug delivery against surra in animal models. ChQS-NPs may be useful for the treatment of surra due to reduced dosages and frequency of administration.

KEYWORDS quinapyramine sulfate, nanoparticles, polymer therapeutics, chitosan, mannitol, *Trypanosoma evansi*

Surra, a hemoprotozoan disease of economic importance in animals, is caused by the flagellated parasite *Trypanosoma evansi*. Although the disease is prevalent in a wide range of animals, few findings indicate their competence to induce disease in humans (1). The disease-infected animals show progressive anorexia and reduced body weight, irregular fever, anemia, edema of dependent body parts, reproductive problems, and nervous symptoms, leading to the death of the infected livestock (2, 3). An aminoquinaldine derivative, quinapyramine sulfate (QS), a commonly used drug for treatment, produces a trypanocidal effect but is often poorly tolerated and causes local reactions as well as general disorders, and sometimes even death, of some animals within minutes of treatment. Horses are known to be highly sensitive to the drug, and at high doses it can produce a toxic reaction within 2 h of administration (4, 5). It is therefore advisable to administer the drug in two to three divided doses at 6-h intervals.

The effective delivery of drug molecules has been a major barrier to desirable therapeutic response against the disease agent. The nanoformulations are known to curtail toxicity and augment the efficiency of the functional components at reduced doses (6, 7). The undesirable side effects of the drug can also be reduced by its sustained and controlled release (8). Previously we encapsulated the drug in the anionic polymer sodium alginate using a double emulsion cross-linking method (9). Although

Received 9 March 2018 **Returned for modification** 29 May 2018 **Accepted** 21 July 2018

Accepted manuscript posted online 13 August 2018

Citation Manuja A, Kumar B, Kumar R, Chopra M, Dilbaghi N, Kumar S, Yadav SC. 2018. Biocompatibility and targeting efficiency of encapsulated quinapyramine sulfate-loaded chitosan-mannitol nanoparticles in a rabbit model of surra. Antimicrob Agents Chemother 62:e00466-18. https://doi.org/10.1128/AAC.00466-18.

Address correspondence to Anju Manuja, amanuja@rediffmail.com.

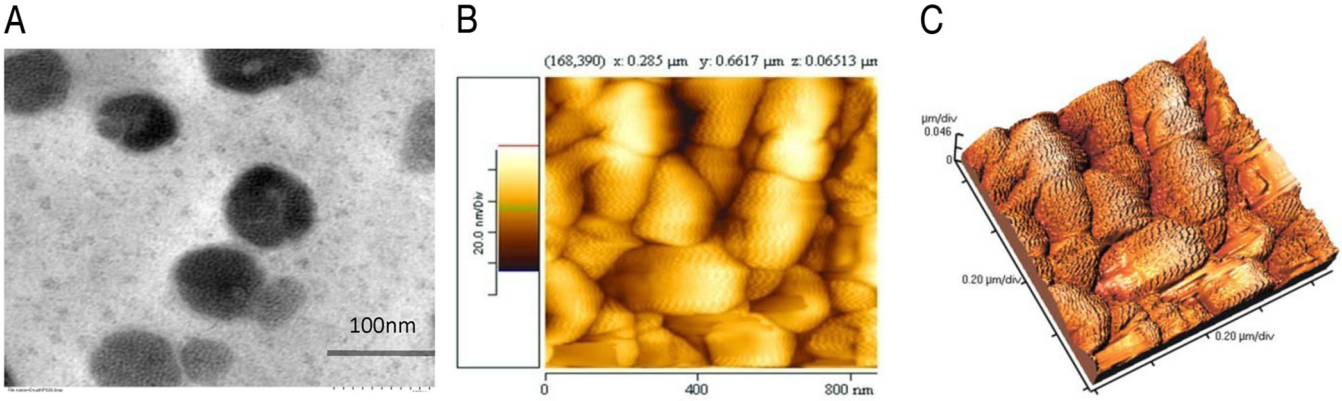

FIG 1 Images of quinapyramine sulfate-loaded chitosan nanoparticles viewed by transmission electron microscopy at 40,000× (A) and atomic force microscopy (B). (C) Three-dimensional view of AFM image.

it was safer than the conventional drug QS at the efficacious doses, at much higher concentrations it was more toxic than the conventional drug. To reduce the toxic effects of the drug, we synthesized a trypanocidal nanoformulation using QS, chitosan (a cationic natural polysaccharide), an anionic tripolyphosphate, and a cryoprotectant, mannitol, employing the ionotropic gelation method. We evaluated the biocompatibility, concentration-dependent safety/cytotoxicity, and genotoxicity of the quinapyramine sulfate-loaded chitosan-mannitol nanoparticles (ChQS-NPs). Further, the targeting ability of ChQS-NPs to counter the parasite in infected rabbits was assessed. The *T. evansi*-infected rabbits experimentally mimic the natural chronic nature of the infection in infected animals (10).

RESULTS AND DISCUSSION

Size, morphology, and charge of ChQS-NPs. The shape and size of the ChQS-NPs, as ascertained by transmission electron microscopy (TEM) and atomic force microscopy (AFM), are shown in Fig. 1A and B. ChQS-NPs were spherical in shape, with particle sizes of less than 100 nm. The three-dimensional (3D) view of surface topology and size of ChQS-NPs observed by AFM is depicted in Fig. 1C as <100 nm. The polydispersity index and the charge of the nanoparticles, determined by Zetasizer (Malvern Instruments Ltd., UK), was 0.557 and +36.4 mV, respectively. Some nanoparticles are stacked and packed together. Therefore, the samples were homogenized before use in the experiment.

Cytotoxicity of ChQS-NPs. The cytotoxicity investigations were performed at various concentrations of ChQS-NPs, and conventional QS was used in the HeLa cell line for ascertaining the biosafety of the nanoparticles. Figure 2 shows the comparison between the cytotoxicity of ChQS-NPs and QS with statistically significant differences ($P < 0.0001$). ChQS-NPs were less toxic than conventional QS and indicated a broad *in vivo* safety margin for the nanoformulations. Fifty percent cytotoxic concentration (CC_{50}) values of QS and ChQS-NPs were 848.33 and 1,336.54 μg/ml, respectively. In our previous study, we observed the CC_{50} of the drug using sodium alginate was 567.54 μg/ml (11). Chitosan proved to be more biocompatible than the other natural polymers.

Genotoxicity of ChQS-NPs. The comet assay was performed using ChQS-NPs, ranging from 10 μg/ml to 5,000 μg/ml (Fig. 3B to E). In the comet assay, the size of the tail increases with the intensity of DNA damage. A tail length of DNA of sample without treatment was compared with that of ChQS-NPs-exposed cells, and the intensity of DNA integrity was ascertained. The cells exposed to ChQS-NPs exhibited a concentration-dependent increase in tail length compared to that of untreated cells (Fig. 3A). No significant DNA damage was observed in untreated cells or cells treated with ChQS-NPs at 10 μg/ml and 312 μg/ml (Fig. 3A to C), while a tail resembling that of a comet, which denotes DNA damage, was observed at concentrations of 2,500 and 5,000 μg/ml of

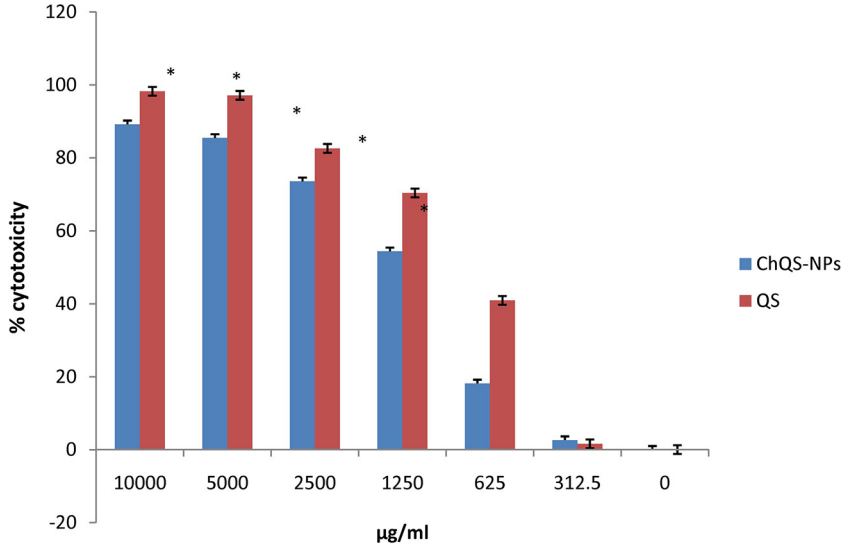

FIG 2 Percent cytotoxicity of different concentrations of ChQS-NPs and QS in HeLa cells after a 65-h incubation at 37°C, using the MTT assay. An asterisk indicates statistical difference ($P < 0.0001$) from the untreated cells (medium alone).

ChQS-NPs (Fig. 3D and E and Table 1) and H_2O_2 at 300 μM concentration (Fig. 3F and Table 1). We observed more DNA damage at higher concentrations (5,000 μg/ml and 2,500 μg/ml) of ChQS-NPs than of QS (Table 1), but when we used concentrations of less than 300 μg/ml, the conventional drug showed more comet tails than ChQS-NPs. Cytotoxicity and genotoxicity investigations showed that the developed ChQS-NPs can be further evaluated for drug delivery in animal models.

Clinical, parasitological, and histopathological evaluation of *T. evansi*-infected rabbits. The rabbits were infected with the parasite by injecting 1×10^5 trypanosomes intramuscularly. Reduced body weight, emaciation, dullness, pale mucous membranes, anemia, lacrimation, corneal opacity, and fluctuating pyrexia were the clinical manifestations observed in *T. evansi*-infected rabbits. The images of rabbits showing discharge from eyes, corneal cloudiness, and swelling of the genitalia are depicted in Fig. 4A. The parasites were visible in the wet blood smears from day 3 to day 5 followed by

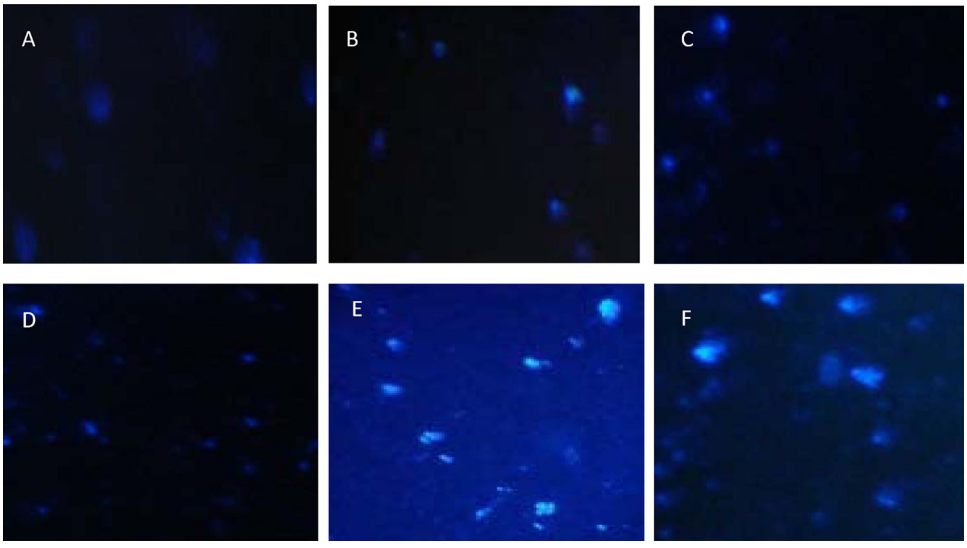

FIG 3 Representative comet assay images of untreated HeLa cells (A) and cells treated with 10 μg/ml ChQS-NPs (B), 312 μg/ml ChQS-NPs (C), 2,500 μg/ml ChQS-NPs (D), 5,000 μg/ml ChQS-NPs (E), and 300 μM H_2O_2 (F).

TABLE 1 Comet tails at different concentrations of QS and QS-chitosan-mannitol-loaded NPs

Sample	Concentration	Comet tails
Negative control (untreated live cells)	0	0
ChQS-NPs	5,000 μg/ml	7
QS	5,000 μg/ml	4
ChQS-NPs	2,500 μg/ml	5
ChQS-NPs	312 μg/ml	1
QS	312 μg/ml	2
ChQS-NPs	10 μg/ml	0
QS	10 μg/ml	0
Positive control (hydrogen peroxide)	300 μM	13

intermittent parasitemia. Inconsistent parasitemia is characteristic of this disease in rabbits and other animals (10, 12). The antibody levels against *T. evansi* before the treatment were measured. The cutoff value of 0.1831 was obtained by the mean absorbance of the uninfected control $\pm$ 3 standard deviations (SD). The samples giving values above 0.1831 were considered positive for *T. evansi* antibodies. Figure 4B shows the graph depicting the cutoff value and absorbance of plasma from infected as well as uninfected rabbits on different days postinfection with statistically significant differences ($P < 0.0001$) from day 7 onwards.

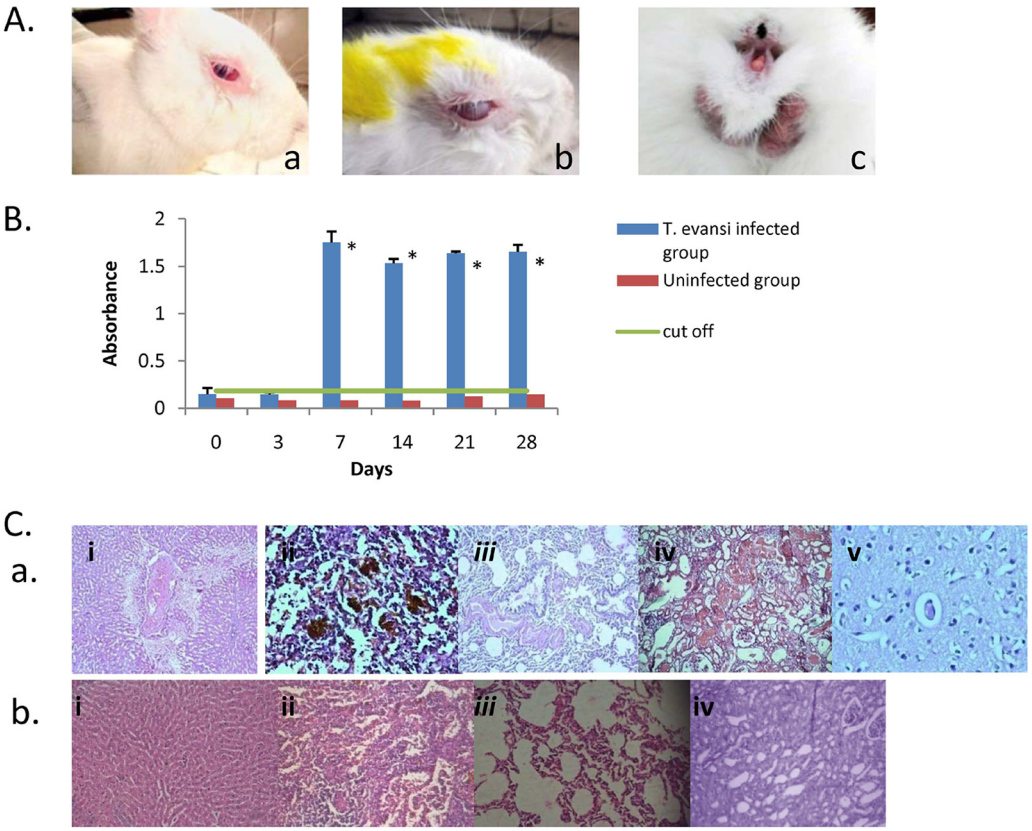

FIG 4 (A) *Trypanosoma evansi*-infected rabbits. The rabbits were infected with 1×10^5 *T. evansi* parasites/animal. Rabbits showed clinical signs of lacrimation (a), corneal opacity (b), and swelling of external genitalia (c). (B) Antibodies against *T. evansi*, determined by ELISA in infected and uninfected rabbits. The rabbits of the infected group were infected with 1×10^5 *T. evansi* parasites/animal. The uninfected rabbits were inoculated with PBS as a negative control. An asterisk indicates statistically significant differences in antibodies against *T. evansi* in infected ($P < 0.001$) and uninfected ($P < 0.0001$) animals. (C, a) Histopathological changes in different tissues of *T. evansi*-infected rabbits (H&E staining was used; magnification, $\times$400). (i) Liver; (ii) spleen; (iii) lung; (iv) kidney; (v) brain. (b) Uninfected rabbits. (i) Liver; (ii) spleen; (iii) lung; (iv) kidney.

At necropsy, we noticed enlarged and necrosed spleen in the rabbits of infected control groups. This is in conformity with the earlier reports documented in donkeys and rabbits (10, 13, 14). Microscopically, the tissue changes in infected rabbits showed hydropic degeneration of liver cells around the central vein, congested blood vessels in the portal triad as well as the central vein, and hemorrhages in hepatic parenchyma, leading to loss of normal hepatic architecture and dilated sinusoids (Fig. 4Cai). Previous research also reported enlarged liver, congestion, areas of necrosis, and destroyed liver cells with the presence of inflammatory cells in the liver of trypanosome-infected rats, rabbits, and ruminants (10, 15–18). Histopathological changes in spleen revealed formation of secondary follicles, hemorrhages, hemosiderin, and edematous fluid (Fig. 4Caii). In lungs, mild to moderate hyperplasia of bronchial epithelium and edema in blood vessels was noticed (Fig. 4Caiii). Histopathological changes in kidney of the infected rabbits revealed mild focal mononuclear cell infiltration, mild hemorrhages, intertubular edema, and congested blood vessels both in medulla and cortex (Fig. 4Caiv). In brain, perineuronal edema and cap congestion in capillaries was observed (Fig. 4Cav). We observed normal architecture of sinusoids in liver, no hemorrhages/hemosiderosis in spleen, normal bronchial epithelium without any hyperplasia and congestion, and no abnormality in medulla and cortex of kidney in uninfected animals (Fig. 4Cbi). The literature suggests trypanosomal diseases induce the formation of systemic antigen-antibody immune complexes, and their deposition in the heart, liver, brain, and kidneys results in tissue damage (19). However, some reports indicated that trypanosomal infections can cause the inflammation of tissues directly (17, 20).

Effect of ChQS-NPs in *T. evansi*-infected rabbits. The rabbits were taken as an experimental model due to the chronic nature of the *T. evansi* infection in this host, mimicking naturally infected animals (10). Forty-five days postinfection, after histopathological evaluation, the remaining eight animals were treated with either QS or ChQS-NPs ($n = 4$ for each treated group). Once the animal is infected, *T. evansi* antibodies persist in the animal body even after treatment or recovery. In our previous study in equines, antibodies persisted up to 6 month posttreatment (12, 21); therefore, this finding should be correlated with clinical signs and parasitological techniques to differentiate between current and treated cases (12). Symptoms of the disease were relieved after 14 days of treatment of the animals, and clearance of the parasites was observed from day 3 to 42 in all rabbits. The representative images of stained slides of blood smears of experimentally infected rabbit and treated rabbit are shown in Fig. 5A and B, respectively. PCR was also employed using TBR1/2 primers, which allows the amplification of repetitive sequence of minichromosome satellite DNA and is considered a gold standard by the OIE for detecting *T. evansi* DNA (22, 23). A representative figure of PCR shows detection of *T. evansi* DNA from *T. evansi*-infected rabbits, depicting bands specific to *T. evansi* at 164 and 384 bp (Fig. 5Ci), whereas the bands were not observed in the DNA samples from infected and treated rabbits (Fig. 5Cii), indicating negative status for *T. evansi* after treatment. A significant increase in hemoglobin values after treatment with conventional drug as well as ChQS-NPs was observed (two-tailed *P* value was less than 0.0001) (Fig. 5D). There was also improvement in the body weight of the treated groups (Fig. 5E). The body temperature decreased significantly (104.05 $\pm$ 0.59°F to 102.6 $\pm$ 0.28°F and 104.2 $\pm$ 0.71°F to 102.8 $\pm$ 0.64°F) in QS and ChQS-NPs treated rabbits on day 3, respectively ($P < 0.05$). The results are shown in Fig. 5F. ChQS-NPs improved the condition of infected rabbits with severe clinical symptoms and prolonged the survivability of these rabbits.

In conclusion, we synthesized biocompatible quinapyramine sulfate-loaded chitosan-TPP-mannitol nanoparticles (ChQS-NPs) to minimize the toxic effects of trypanocidal QS and simultaneously ensured enhanced efficacy at reduced doses against *T. evansi*. The results shown here give a proof of principle for the efficacy of ChQS-NPs at reduced doses of 1 mg/kg of body weight in severely *T. evansi*-infected rabbits. These encouraging results support further studies to demonstrate effectiveness in large animals.

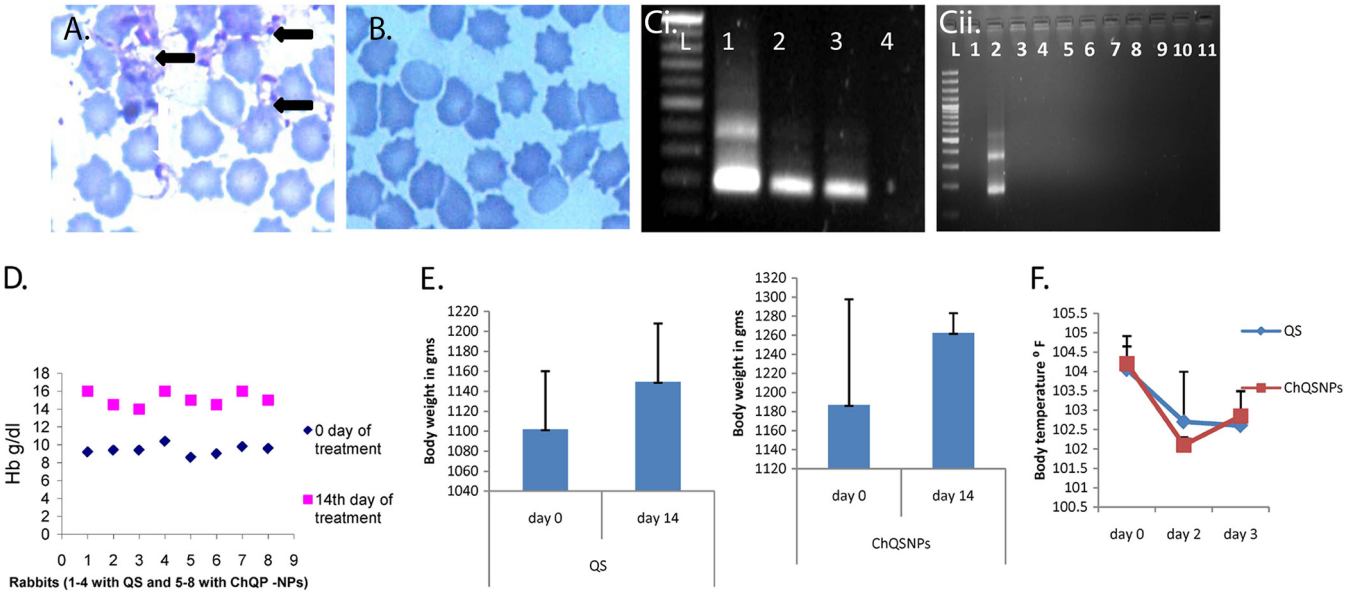

FIG 5 Effect of quinapyramine sulfate-loaded chitosan nanoparticles on *T. evansi* in rabbits. (A) Giemsa-stained blood smear of rabbit experimentally infected with *T. evansi*. The white arrow shows the parasite *T. evansi*, and black arrows depict bunches of parasites. (B) Giemsa-stained blood smear of experimentally infected and treated rabbit. Parasite was not detected in blood smear of the infected and treated rabbit. (C, i) Representative PCR image showing detection of *T. evansi* DNA (lane L, ladder; lanes 1, 2, and 3, DNA from *T. evansi*-infected rabbit; lane 4, DNA from infection-negative rabbit. (ii) Lane 1, DNA from infection-negative rabbit; lane 2, DNA from *T. evansi*-infected rabbit; lanes 3 to 11, DNA from infected and treated rabbits. (D) Percent hemoglobin levels. (E) Body weight. (F) Rectal temperature of infected rabbits before and after treatment with QS and ChQS-NPs.

MATERIALS AND METHODS

Synthesis of ChQS-NPs. ChQS-NPs were synthesized using the drug QS, the polymer chitosan (CS), tripolyphosphate (TPP), and mannitol nanomatrix using ionotropic gelation. CS (deacetylated chitin, 75 to 85% deacetylation) was added at 0.8 to 1 g in 100 ml of 2%, vol/vol, acetic acid and stirred for 6 h. TPP solution (92 to 138 mg in 100 ml dry weight) containing 50 mg of QS was pipetted in drops slowly to the previously prepared CS solution, with continuous stirring. The mixture was further mixed on a stirrer for 24 h. The NPs were collected by centrifugation at 15,000 rpm for 20 min and rinsed twice with distilled water using the same speed for 10 min. Finally, the NPs were suspended in 1.5 to 5%, wt/vol, D-mannitol solution and probe sonicated (15-s on pulse and 20-s off pulse) for a total of 20 min and lyophilized at −90°C.

Morphology and size. The morphology and size of the ChQS-NPs were ascertained by a transmission electron microscope (TEM; H-7650; Hitachi). The grids for TEM were prepared as described previously (9) and viewed under the microscope with the high-contrast imaging mode at 80 kV. Atomic force microscopy (AFM) was performed to investigate the outward morphology of nanoparticles along with size distribution. Formulated nanoparticles were dispersed in distilled water (1 mg/ml). The AFM images were viewed under a Veeco di-CP-II (Veeco, USA) operating in tapping noncontact mode in air.

Cell culture. We cultured the HeLa cell line in Dulbecco's modified Eagle's medium (DMEM) containing 10% fetal bovine serum (FBS), 10 mM HEPES, 2 mM L-glutamine, 25 mM sodium bicarbonate, 10 mg/ml streptomycin, 10,000 U/ml penicillin, and 25 μg/ml amphotericin B. The cells were maintained at 37°C under 5% CO_2.

Cytotoxicity studies. The biocompatibility of the ChQS-NPs was ascertained as described previously (11) by culturing 200 μl of 1 × 10^5/ml cell culture into each well of 96-well plates for 24 h at 37°C and 5% CO_2. Cells then were treated with various concentrations of ChQS-NPs and hydrogen peroxide (H_2O_2; 300 μM) as a positive control. After incubation for 65 h at 37°C, as described earlier (11), the reagent 3-(4, 5-dimethyl thiazolyl-2)-2,5-diphenyl tetrazolium bromide (MTT; 10 μl of 1 μg/μl per well; Sigma-Aldrich, USA) was added to the replaced medium and incubated for 4 h under the same conditions. MTT was reduced to the purple-colored insoluble formazan, which was solubilized in 100 μl of dimethyl sulfoxide (DMSO). The optical density (OD) was read at 570 nm using a plate reader. The background OD of the samples measured at 690 nm was subtracted from the OD taken at 570 nm, and we determined the 50% cytotoxic concentration (CC_{50}) with respect to untreated cells.

Genotoxicity of ChQS-NPs. The alkaline comet test was performed to determine the effect of ChQS-NPs on DNA (11). Briefly, the culture of 1 × 10^5/ml HeLa cells (500 μl/well) in 24-well plates was treated with various concentrations of ChQS-NPs and positive-control H_2O_2. The treated cultures were incubated for 65 h at 37°C in 5% CO_2, washed, resuspended in cold phosphate-buffered saline (PBS), and mixed with comet agarose (at 1:10). Immediately, 75 μl/well was transferred to the comet slides (Chromous Biotech, Bangalore, India) that were air dried in the dark at 4°C for 15 min and transferred to cold lysis buffer for 60 min under the same conditions of temperature and darkness. Alkaline electrophoresis was performed by applying 1 V/cm and 300 mA to the chamber for 15 to 30 min. The slides were

rinsed with cold water-ethanol and air dried. Finally, we stained the slides with DNA dye, and the tail length of sample DNA was observed under an epifluorescence microscope using a fluorescein isothiocyanate filter.

Experimentally induced infection of rabbits with *T. evansi* parasite. The experiments on animal models were conducted as per the guidelines provided by the Committee for the Purpose of Control and Supervision of Experiments on Animals (CPCSEA), Government of India. The animal experimentation was endorsed by the Institute Animal Ethics Committee of ICAR-National Research Centre on Equines (ICAR-NRCE), Hisar, Haryana, India. *T. evansi* parasites, maintained in a frozen state at ICAR-NRCE, were propagated in albino mice by injecting 1×10^4 *T. evansi* parasites intraperitoneally. Peripheral parasitemia was examined daily in the blood collected from mouse tails. After 6 days, 10 New Zealand White rabbits (age of approximately 3 to 5 months), procured from a disease-free small-animal house, were infected intramuscularly with 1×10^5 trypanosomes and examined daily for parasitemia. Four rabbits were kept as an uninfected negative control. The rabbits were housed individually in stainless steel mesh cages (3-ft^2 area) under ambient temperature (20 $\pm$ 2°C). The cages contained feeder and water bowls for *ad libitum* feeding.

Measurement of antibodies against *T. evansi*. The *T. evansi*-specific antibodies in infected and uninfected rabbits were estimated by enzyme-linked immunosorbent assay (ELISA) as previously described (10, 12, 21). Briefly, ELISA plates were coated with 0.5 μg of *T. evansi* antigen prepared from whole-cell lysate in 0.1 M carbonate-bicarbonate buffer (pH 9.6), kept overnight at 4°C, and further blocked with 5% skimmed milk in PBST (PBS plus 0.05% Tween 20) for 1 h at 37°C. The plates were washed six times with PBST, and equal quantities of plasma samples (1:100 in blocking solution) were pipetted to the designated wells and further incubated for 1 h at the same temperature. After washings, equal quantities of goat anti-rabbit IgG-horseradish peroxidase conjugate (Sigma) at a 1:5,000 dilution was pipetted as described above and incubated under the same conditions. After six washings, substrate solution (tetramethylbenzidine [1:20 TMB-H_2O_2]) was added. Subsequently, the reaction was terminated with 1 M sulfuric acid after 10 min. The absorbance was taken at 450 nm by an ELISA plate reader (BioTek, USA). The mean OD $\pm$ 3 SD for negative plasma samples was taken as the cutoff value to quantify the results.

Histopathological evaluation. After the appearance of severe clinical signs, the rabbits were either sacrificed for histopathological investigations or treated with ChQS-NPs and QS after 45 days of infection. The rabbits were sacrificed by infusing sodium thiopentone intravenously. The animals were sacrificed quickly and without pain in a peaceful atmosphere. The pieces of tissues (liver, lung, spleen, kidney, and brain) were collected and fixed in 10% neutral buffered formalin. The tissues were processed and stained for histopathological examination as described earlier (10). Hematoxylin-and-eosin (H&E)-stained slides were observed microscopically to see the histological changes due to *T. evansi* infection.

Efficacy of ChQS-NPs in *T. evansi*-infected rabbits. Forty-five days postinfection, after the development of severe clinical signs, the animals were divided into the following groups for intramuscular treatment with drugs: group 1, ChQS-NPs at 1 mg/kg ($n = 4$) in three divided doses (0.33 mg/kg) at a 12-h interval; group 2 ($n = 4$), conventional drug QS at the recommended dose (5 mg/kg). The body temperature and clinical symptoms of the rabbits of all groups were documented daily, whereas the body weight of the rabbits was recorded once a week. The parasitemia was observed through wet blood-smeared slides. The Giemsa-stained thin blood smears were also examined for the presence of parasites.

The DNA was isolated from rabbit blood using a DNeasy kit (Qiagen, GmBH, Hilden, Germany) per general instructions from the company. The PCR was performed using TBR1/2 primers, recommended as a gold standard by the OIE for detection of *T. evansi* DNA (22, 23).

Statistical analysis. The results are presented as means $\pm$ SD from replicated experiments. Any variation among the experimental groups was analyzed by Student *t* test using GraphPad software online. The significant differences among the groups were examined at a *P* value of <0.0001.

ACKNOWLEDGMENTS

Financial support from the Department of Science and Technology, Government of India, in the form of a research project, "Synthesis, characterization, and evaluation of drug-loaded nano-formulations against *Trypanosoma evansi* in animal model" (grant no. SR/NM/NS-1064/2011), under the Nano Mission program, is gratefully acknowledged.

We thank the late Parveen Kumar for providing help in *T. evansi* experiments.

REFERENCES

1. Joshi PP, Shegokar VR, Powar RM, Herder S, Katti R. 2005. Human trypanosomosis caused *Trypanosoma evansi* in India: the first case report. Am J Trop Med Hyg 73:491–495.
2. Rathore NS, Manuja A, Manuja BK, Choudhary S. 2016. Chemotherapeutic approaches against *Trypanosoma evansi*: retrospective analysis, current status and future outlook. Curr Top Med Chem 16:2316–2327. https://doi.org/10.2174/1568026616666160413125802.
3. Yadav SC, Jaideep K, Gupta AK, Jerome A, Prabhat K, Rajender K, Kanika T, Ritesh K. 4 December 2016. Parasitological, biochemical and clinical observations in ponies experimentally infected with *Trypanosoma evansi*. J Exp Biol Agric Sci https://doi.org/10.18006/2016.4(Spl-4-EHIDZ).S144.S150.
4. Finelle P. 1983. African animal trypanosomosis, p 12–20. FAO animal production and health paper, world animal review, vol 37. FAO, United Nations, Rome, Italy.
5. Hayat CS, Khan QM, Hayat B, Iqbal Z. 1987. Studies of the efficacy and

safety of quinapyramine sulphate against trypanosomosis in naturally infected horses and donkeys. Pak J Agric Sci 24:295.
6. Aprahamian MM, Michel CC, Humbert WW, Devissaguet JP, Damge CC. 1987. Transmucosal passage of poly (alkylcyanoacrylate) nanocapsules as a new drug carrier in the small intestine. Biol Cell 61:69–76. https://doi.org/10.1111/j.1768-322X.1987.tb00571.x.
7. Manuja A, Kumar B, Singh RK. 2012. Nanotechnology developments: opportunities for animal health and production. Nanotech Dev 2:e4. https://doi.org/10.4081/nd.2012.e4.
8. Calvo P, Gouritin B, Chacun H, Desmaele D, Angelo JD, Noel JP, Georgin D, Fattal E, Andreux JP, Couvreur P. 2001. Long-circulating PEGylated polycyanoacrylate nanoparticles as new drug carrier for brain delivery. Pharm Res 18:1157–1166. https://doi.org/10.1023/A:1010931127745.
9. Manuja A, Kumar S, Dilbaghi N, Bhanjana G, Chopra M, Kaur H, Kumar R, Kumar B, Singh SK, Yadav SC. 2014. Quinapyramine sulfate-loaded sodium alginate nanoparticles shows enhanced trypanocidal activity. Nanomedicine (Lond) 9:1625–1634. https://doi.org/10.2217/nnm.13.148.
10. Kumar P, Kumar R, Manuja BK, Singha H, Sharma A, Virmani N, Yadav SC, Manuja A. 2015. CpG-ODN class C mediated immunostimulation in rabbit model of *Trypanosoma evansi* infection. PLoS One 10:e0127437. https://doi.org/10.1371/journal.pone.0127437.
11. Manuja A, Kumar B, Chopra M, Bajaj A, Kumar R, Kumar S, Dilbaghi N, Bhanjana G, Kaur H, Kumar B, Singh SK, Yadav SC. 2016. Cytotoxicity and genotoxicity of a trypanocidal drug quinapyramine sulfate loaded-sodium alginate nanoparticles in mammalian cells. Int J Biol Macromol 8:146–155. https://doi.org/10.1016/j.ijbiomac.2016.03.034.
12. Yadav SC, Kumar R, Manuja A, Goyal L, Gupta AK. 2014. Early detection of *Trypanosoma evansi* infection and monitoring of antibody levels by ELISA following treatment. J Parasit Dis 38:124–127. https://doi.org/10.1007/s12639-012-0204-2.
13. Cadioli FA, Marques LC, Machado RZ, Alessi AC, Aquino LP, Barnabe PA. 2006. Experimental *Trypanosoma evansi* infection in donkeys: hematological, biochemical and histopathological changes. Arq Bras Med Vet Zootec 58:749–756. https://doi.org/10.1590/S0102-09352006000500008.
14. Siva Jothi S, Rayulu VC, Sujatha K, Reddy S, Amaravathi P. 2013. Histopathological observations in rabbits experimentally infected with *Trypanosoma evansi*. J Adv Vet Res 3:122–126.
15. Biswas D, Choudhury A, Misra KK. 2001. Histopathology of *Trypanosoma*, *Trypanozoon evansi* infection in bandicoot rat. I. Visceral organs. Exp Parasitol 99:148–159. https://doi.org/10.1006/expr.2001.4664.
16. Dargantes AP, Reid SA, Copman DB. 2005. Experimental *Trypanosoma evansi* infection in the goat. I. Clinical signs and clinical pathology. J Comp Pathol 133:261–266.
17. Damayanti R, Graydon RJ, Ladds PW. 1994. The pathology of experimental *Trypanosoma evansi* infection in the Indonesian buffalo (*Bubalus bubalis*). J Comp Pathol 110:237–252. https://doi.org/10.1016/S0021-9975(08)80277-0.
18. Tizard IR. 1998. Imunologia veterinária–uma introdução, 5th ed. Roca, São Paulo, Brazil.
19. Sudarto MW, Tabel H, Haines DM. 1990. Immunohistochemical demonstration of *Trypanosoma evansi* in tissues of experimentally infected rats and a naturally infected water buffalo (*Bubalus bubalis*). J Parasitol 76:162–167. https://doi.org/10.2307/3283007.
20. Ngeranwa JJ, Gathumbi PK, Mutiga ER, Agumbah GJ. 1993. Pathogenesis of *Trypanosoma* (*brucei*) *evansi* in small east African goats. Res Vet Sci 54:283–289. https://doi.org/10.1016/0034-5288(93)90124-X.
21. Kumar R, Kumar S, Khurana SK, Yadav SC. 2013. Development of an antibody-ELISA for seroprevalence of *Trypanosoma evansi* in equids of north and north-western regions of India. Vet Parasitol 196:251–257. https://doi.org/10.1016/j.vetpar.2013.04.018.
22. Masiga K, Smyth AJ, Hayes P, Bromidge TJ, Gibson WC. 1992. Sensitive detection of trypanosomes in tsetse flies by DNA amplification. Int J Parasitol 22:909–918. https://doi.org/10.1016/0020-7519(92)90047-O.
23. Kankar SK, Kumar R, Goyal SK, Gaur DK, Sharma P, Bera BC, Garg R, Kumar S, Yadav SC. 2016. Quantification of *Trypanosoma evansi* parasitic load in experimentally infected mice using real time PCR assay and its comparative evaluation with conventional parasitological techniques. Ind J Anim Sci 86:1378–1384.